

# CO<sub>2</sub> SORPTION USING Na<sub>2</sub>CO<sub>3</sub>/Al<sub>2</sub>O<sub>3</sub> SORBENT WITH VARIOUS FLOW PATTERNS OF FIXED/FLUIDIZED BED REACTORS

## Article history

Received

19 June 2015

Received in revised form

13 September 2015

Accepted

12 December 2015

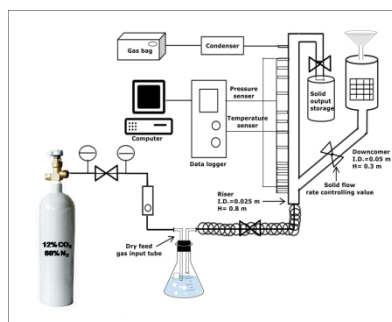
Nathphatsorn Jongartklang<sup>a</sup>, Ratchanon Piemjaiswang<sup>a</sup>, Pornpote Piumsomboon<sup>a</sup>, Benjapon Chalermisinsuwan<sup>a,b\*</sup>

\*Corresponding author  
benjapon.c@chula.ac.th

<sup>a</sup>Department of Chemical Technology, Faculty of Science, Chulalongkorn University, 254 Phayathai Road, Patumwan, Bangkok 10330, Thailand

<sup>b</sup>Center of Excellence on Petrochemical and Materials Technology, Chulalongkorn University, 254, Phayathai Road, Patumwan, Bangkok 10330, Thailand

## Graphical abstract



## Abstract

In this study, the carbon dioxide sorption using solid sorbent (sodium carbonate supported on alumina) in fixed and fluidized bed reactors was investigated. The key objective was to examine the carbon dioxide concentration profile or breakthrough curve (as well as capture capacity) and carbon dioxide sorption kinetic parameters with various flow regimes/flow patterns. The basic information for the sorption kinetic parameter computation was the breakthrough curve under different flow operating conditions. From the results, all the breakthrough curves were constant at the beginning stage then it decreased with the sorption time. The fixed bed gave longest sorption time. All the carbon dioxide gas was not captured in the fast fluidization flow regime. The turbulent fluidization flow regime exhibited highest carbon dioxide capture capacity. In addition, the employed deactivation kinetic model fitted well with the obtained experimental information. The initial sorption and deactivation reaction rate constants were the highest at the turbulent fluidization flow regime.

**Keywords:** Breakthrough curve, carbon dioxide, deactivation model, flow regimes/patterns, sodium carbonate

© 2016 Penerbit UTM Press. All rights reserved

## 1.0 INTRODUCTION

Carbon dioxide (CO<sub>2</sub>) is known as a major cause of global warming problem due to their ability to maintain the heat inside the earth atmosphere [1]. Recently, the fluidization technology using dry solid sorbent has been considered as an alternative for reducing CO<sub>2</sub> release [2-4]. For conventional gas-solid particle flow, the flow operating condition can be divided into five different regimes/patterns with the increasing of gas inlet velocity [5]. Each regime has its

own distinct characteristic [6]. Sodium carbonate (Na<sub>2</sub>CO<sub>3</sub>) is promisingly proposed to use as a solid sorbent because it can easily adsorb and regenerate using low temperature and economically employed when comparing to the other solid sorbents [7]. The fundamental theory about adsorption of CO<sub>2</sub> on Na<sub>2</sub>CO<sub>3</sub> can be found in the previous studies [7-11]. From the literature, the research study about CO<sub>2</sub> sorption using solid sorbents has paid attention on two topics: solid sorbent development and process system

improvement [8-9]. For the solid sorbent development,  $\text{Na}_2\text{CO}_3$  was performed as the active component of the solid sorbent [7]. To improve the sorption efficiency and the attrition resistance of the solid sorbent,  $\text{Na}_2\text{CO}_3$  was prepared on various supporting materials, such as activated carbon, silica, vermiculite and alumina [10-11]. For the process system improvement, the  $\text{CO}_2$  capture performance with various system variables such as gaseous composition, operating pressure and operating temperature were mainly evaluated in fixed bed reactor [12-14]. However, there are still many problems that need to be solved. The understanding of  $\text{CO}_2$  capture behavior and  $\text{CO}_2$  sorption kinetic parameters will help engineers and technologists to better design the commercial chemical reactor.

About the reaction kinetic study, the deactivation model was effectively used to illustrate the decreasing in activity of alkali-metal carbonate during chemical reaction of various alkali-metal carbonates with  $\text{CO}_2$  when comparing to the other chemical kinetic models, the homogeneous model and the shrinking-core model [15-18]. Though, most reaction kinetic studies on the  $\text{CO}_2$  capture using alkaline-metal carbonate were mainly performed in the thermogravimetric analyzer which then encountered the mass transfer limitation effect. Recently, Lee *et al.* [19] and Guo *et al.* [20] investigated the carbonation reaction kinetic behaviors of alkaline-metal carbonate generated by calcination of alkaline-metal bicarbonate with a pressurized thermogravimetric and fixed bed apparatus, respectively.

The deactivation model was therefore selected to calculate the kinetic parameters of carbonation reaction for sodium carbonate supported on alumina ( $\text{Na}_2\text{CO}_3/\text{Al}_2\text{O}_3$ ) in fixed and fluidized bed reactors. In addition, the effect of flow regimes/flow patterns on the  $\text{CO}_2$  capture behavior and  $\text{CO}_2$  sorption kinetic parameters was discussed based on the system hydrodynamics.

## 2.0 EXPERIMENTAL

### 2.1 Solid Sorbent Preparation

In this study, the pure  $\text{Na}_2\text{CO}_3$  was impregnated on porous alumina support ( $\text{Al}_2\text{O}_3$ ) for using as the solid sorbents. The aqueous solution containing five grams of  $\text{Na}_2\text{CO}_3$  in 25 ml of de-ionized water was added with five grams of support. Then, the solution was mixed in an orbital-shaker for 24 hours at room temperature. After the mixing, the obtained solution was dried at  $105^\circ\text{C}$  in a vacuum oven and calcined at  $300^\circ\text{C}$  with the ramping temperature rate of  $3^\circ\text{C}/\text{min}$  in a furnace for 4 hours. The surface area of solid sorbent was determined using Micromeritics 2020 apparatus (BET) while the quantity of alkaline metal impregnated was quantified by using Energy Dispersive X-Ray Fluorescence Spectrometer (EDX). The other physical properties of  $\text{Na}_2\text{CO}_3/\text{Al}_2\text{O}_3$  solid sorbent are sum up in Table 1.

### 2.2 Apparatus

The  $\text{CO}_2$  sorption was experimented in a laboratory scale fixed bed and fluidized bed reactors as displayed in Figure 1. The riser section, made from glass, had 0.025 m inside diameter and 0.80 m height while the downcomer section, made from poly-vinylchloride (PVC), had 0.050 m inside diameter and 0.30 m height. The solid sorbent storage was employed to collect entrained solid sorbents above the riser section. The controlling valve was employed to regulate the feeding or returning flow of solid sorbents to the riser section. The temperature and pressure taps were placed along the riser height to evaluate the system temperature and pressure, respectively. The solid sorbent flow regimes/flow patterns were explored by considering the solid concentration or volume fraction ( $\epsilon_s$ ) along the riser height. The  $\epsilon_s$  was determined using the obtained pressure drop,  $\Delta P$ , measuring at the mounted pressure taps. By discarding the acceleration flow contribution effect and wall friction effect, the relationship  $\Delta P = \rho_s(\epsilon_s)gH$  then valid (where  $g$  and  $H$  being the gravitational force acceleration and the length between two successive pressure taps, respectively).

**Table 1** Prepared  $\text{Na}_2\text{CO}_3/\text{Al}_2\text{O}_3$  solid sorbent physical properties

Solid sorbent property	Value
Surface area of solid sorbent ( $\text{m}^2/\text{g}$ )	105.4
Actual weight of $\text{Na}_2\text{CO}_3$ impregnated on $\text{Al}_2\text{O}_3$ (wt%)	10
Diameter of solid sorbent ( $d_p$ , $\mu\text{m}$ )	150
Density of solid sorbent ( $\rho_s$ , $\text{kg}/\text{m}^3$ )	2,545

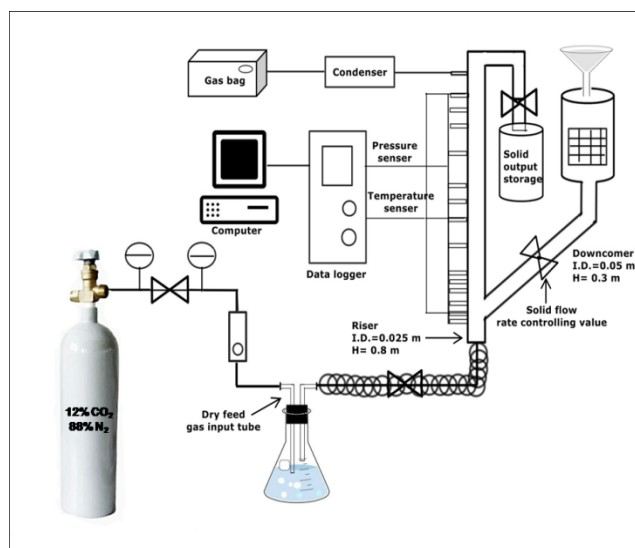


**Figure 1** The reactor system used in this study

### 2.3 Flow Regime/Pattern Characterization

The wide range of gas velocities from 0.02 to 2.30 m/s was investigated in this study. Five different flow regimes/patterns with the increasing of gas velocity were operated. These include two different operations which are the circulating operation system and the non-circulating operation system. The non-circulating operation system was consisting of four unique flow regimes/flow patterns: fixed bed, bubbling fluidized bed, slugging fluidized bed and turbulent fluidized bed. However, the small amount of bed material was circulated in the turbulent fluidized bed or fluidization regime. The circulating operation system was run in fast fluidized bed or fluidization regime. All the used flow regimes/flow patterns were previously verified the system hydrodynamics in our preceding study [21]. Table 2 presents the operating conditions with different gas velocities.

### 2.4 CO<sub>2</sub> Sorption Procedure

For the CO<sub>2</sub> sorption study, the 40 g and 200 g of Na<sub>2</sub>CO<sub>3</sub>/Al<sub>2</sub>O<sub>3</sub> solid sorbent were placed into the riser section for non-circulating and circulating operation systems, respectively. The inlet gas composition, which was measured by online sensor, was prepared as the simulated flue gas composition. The other experimental conditions of flow regimes/patterns in fixed and fluidized bed reactors are shown in Table 3. After the sorption, the gas at the top of the riser section was sampling to measure the quantity of CO<sub>2</sub> in mixture gas using gas chromatography column (GC).

### 2.5 Kinetic Parameters Calculation

As stated in the introduction, the deactivation model was used. In this model, the diffusion resistance creating from the occurrence of the product deposition on the reactant is the reason for a decreasing in the rate of chemical reaction. The considerable changes in the surface area, the pore structure and the activity of solid reactant are then arisen. All the changes are included in a deactivation model. When the deactivation of the solid sorbent is specified to be first-order with respect to the concentration of CO<sub>2</sub> gas and the solid active sites, after solving iterative procedure of the obtained equation as described and derived by Park *et al.* [16], it can be found that:

$$\frac{C}{C_0} = \exp \left[ I - \frac{\exp \left( \frac{k_s W}{Q_s} (1 - \exp(-k_d t)) \right)}{1 - \exp(-k_d t)} \right] \exp(-k_d t) \quad (1)$$

where  $t$  is time,  $Q_0$  is gas flow rate,  $W$  is weight of solid sorbent,  $C$  is CO<sub>2</sub> outlet concentration and  $C_0$  is CO<sub>2</sub> inlet concentration. Therefore, the two kinetic parameters of  $k_0$  (initial sorption rate constant) and  $k_d$  (deactivation rate constant) are then calculated from the CO<sub>2</sub> concentration profile.

**Table 2** The operations of flow regimes/patterns

Fluidization operation system	Solid sorbent loading (g)	Flow regime / flow pattern	Inlet gas velocity (m/s)
Non-circulating	40	Fixed bed	0.02
		Bubbling	0.18
		Slugging	0.32
		Turbulent	0.84
Circulating	200	Fast fluidization	2.30

**Table 3** The experimental conditions of CO<sub>2</sub> sorption in fixed bed and fluidized bed reactors

Condition	CO <sub>2</sub> sorption
System temperature (°C)	60
System pressure (atm)	1
Gas composition (vol.%)	CO <sub>2</sub> : 12, H <sub>2</sub> O: 19.5, N <sub>2</sub> : balance
Mole fraction of H <sub>2</sub> O (water vapor) to CO <sub>2</sub> (-)	1.60

## 3.0 RESULTS AND DISCUSSION

### 3.1 Carbonation Behaviors

The flow regimes/flow patterns effect on CO<sub>2</sub> breakthrough curves of Na<sub>2</sub>CO<sub>3</sub>/Al<sub>2</sub>O<sub>3</sub> solid sorbent in fixed bed and fluidized bed reactors at system temperature of 60°C and system pressure of 1 atm in 12 vol.% of CO<sub>2</sub> and 19.5 vol.% of H<sub>2</sub>O is shown in Figure 2.

For the CO<sub>2</sub> concentration profile under fixed bed flow pattern, the CO<sub>2</sub> breakthrough curve was constant at the beginning stage then it progressively decreased with the sorption time. For bubbling fluidization regime, the trend of CO<sub>2</sub> concentration curve was comparable to the one with fixed bed flow pattern. However, the constant period of CO<sub>2</sub> breakthrough curve in bubbling fluidized bed flow regime was less than the one in fixed bed flow pattern. This is because the inlet gas velocity of bubbling fluidized bed is higher than that of fixed bed. For slugging and turbulent fluidization regimes, the CO<sub>2</sub> breakthrough curve increased sharply from the beginning stage with the increasing of sorption time because the system residence time through the bed is inadequate for the reactant gas to transfer onto the surface of solid sorbents. Although the system residence time in turbulent fluidization flow regime was lower than the slugging fluidization flow regime, the CO<sub>2</sub> sorption under turbulent fluidization flow regime was higher. The large contacting surface area of gas-solid sorbent inside the turbulent fluidized bed flow regime is the reason for the obtained phenomenon. When the solid sorbents were performed in fast

fluidization flow regime, the solid sorbents were elutriated by the high inlet gas velocity and returned to the feeding section at the bottom of the riser. It took 6 min for all 200 grams of solid sorbent to pass through the riser section. During first sorption cycle or 0 to 6 min, the fresh solid sorbent adsorbed about 80 percent ( $C_A/C_{A0} \approx 0.20$ ) of  $\text{CO}_2$  in the feed because the extremely high operating gas velocity. The competition between the effect of gas-solid sorbent contacting surface area and system residence time (or solid sorbent elutriation) on  $\text{CO}_2$  capture is found in this flow regime. After 6 min, the sorption reaction of  $\text{Na}_2\text{CO}_3/\text{Al}_2\text{O}_3$  solid sorbents gradually decreased or the  $\text{CO}_2$  concentration gradually increased due to the returning of employed solid sorbents.

Figure 3 shows the  $\text{CO}_2$  capture capacity (the ratio of the overall amount of  $\text{CO}_2$  sorption per the amount of active component on solid sorbent) at different flow regimes of  $\text{Na}_2\text{CO}_3/\text{Al}_2\text{O}_3$  solid sorbent in fixed and fluidized bed reactors at system temperature of  $60^\circ\text{C}$  and system pressure of 1 atm in 12 vol.% of  $\text{CO}_2$  and 19.5 vol.% of  $\text{H}_2\text{O}$ . The fixed bed, slugging and fast fluidizations showed poor  $\text{CO}_2$  capture capacity at about 97-158 mg  $\text{CO}_2/\text{g Na}_2\text{CO}_3$  while the turbulent and bubbling fluidizations showed good  $\text{CO}_2$  capture capacity at about 190-194 mg  $\text{CO}_2/\text{g Na}_2\text{CO}_3$ . When considering the  $\text{CO}_2$  breakthrough curve or  $\text{CO}_2$  concentration profile as shown in Figure 2, the fixed bed flow pattern gave the highest sorption time. However, the achieved  $\text{CO}_2$  capture capacity was not the highest in this flow pattern. The reason is because the solid sorbent packing among each other causes the active site loss of the solid sorbent. In bubbling fluidization regime, the  $\text{CO}_2$  capture capacity of solid sorbents showed that higher gas-solid sorbent contacting surface area will give better the  $\text{CO}_2$  capture capacity of solid sorbents. For the remaining fluidization flow regimes, the solid sorbents

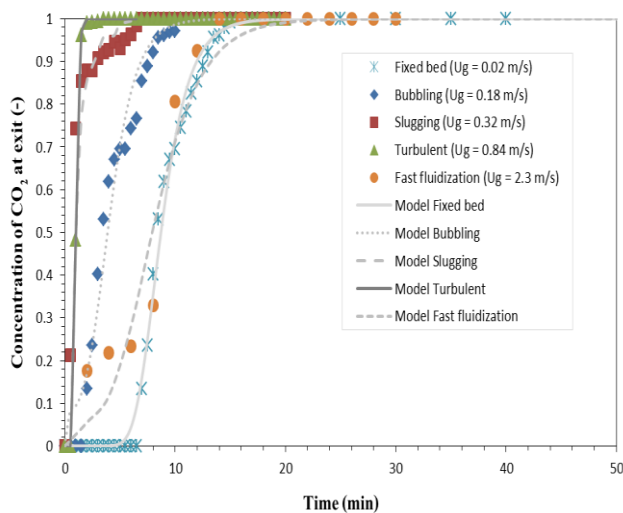


**Figure 2** The effect of various flow regimes/flow patterns on breakthrough curve of  $\text{CO}_2$  concentration at system temperature of  $60^\circ\text{C}$  and system pressure of 1 atm in 12 vol.% of  $\text{CO}_2$  and 19.5 vol.% of  $\text{H}_2\text{O}$

could not capture all the  $\text{CO}_2$  gas even at the early stage. Considering the  $\text{CO}_2$  capture capacity of solid sorbents, the slugging and fast fluidization flow regimes showed lowest capture capacity of solid sorbents because the large gas bubble forming in the slugging fluidization regime and low system residence time in the fast fluidization regime. The turbulent fluidization regime reflected the promising  $\text{CO}_2$  capture capacity. The proper solid sorbent elutriation and system back-mixing are the explanation for this situation [5].

### 3.2 Carbonation Chemical Reaction Kinetics

To obtain chemical reaction kinetic parameters ( $k_0$  and  $k_d$ ), the regression fitting was performed using Equation (1) with non-linear least square technique [16]. Figure 2 also displays the regression results of the real experimental data by the deactivation model. The selected deactivation model could precisely predict the breakthrough behaviors for all the reaction of  $\text{Na}_2\text{CO}_3/\text{Al}_2\text{O}_3$  and  $\text{CO}_2$ . Table 4 summarizes the kinetic parameters for all flow regimes/patterns of  $\text{Na}_2\text{CO}_3/\text{Al}_2\text{O}_3$  solid sorbent in fixed and fluidized bed reactors at system temperature of  $60^\circ\text{C}$  and system pressure of 1 atm in 12 vol.% of  $\text{CO}_2$  and 19.5 vol.% of  $\text{H}_2\text{O}$ . As can be seen from the results, the sorption kinetic parameters were greatly depending on the flow regime/pattern performing inside the system. In general, the chemical reaction kinetic parameters are those that describe the reaction rate and they then should be the same irrespective of the reactor type. However, the kinetic models in this study were the overall or simplified kinetic models including mass transfer and chemical reaction resistances. Because the obtained kinetic parameters were different in each type of fluidization flow regime, it can be concluded that mass transfer resistance occurred and governed these systems.

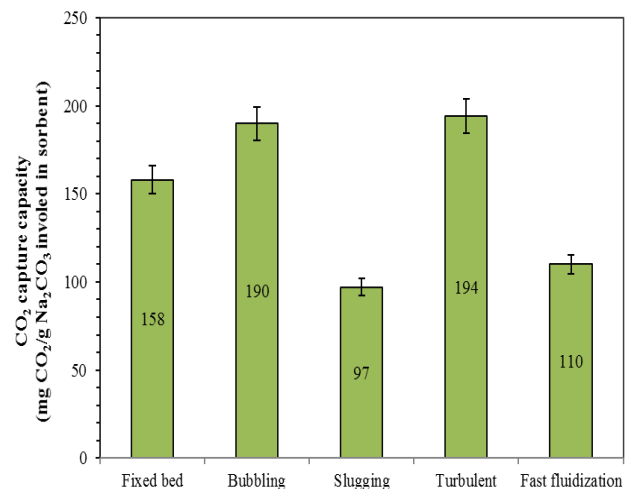
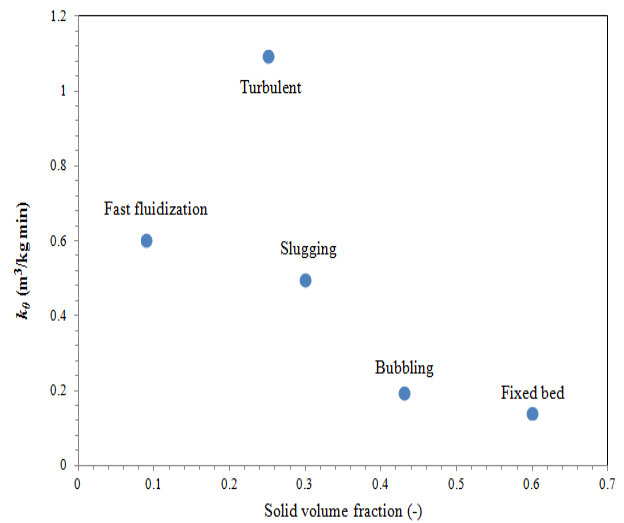


**Figure 3** The effect of various flow regimes/flow patterns on  $\text{CO}_2$  capture capacity at system temperature of  $60^\circ\text{C}$  and system pressure of 1 atm in 12 vol.% of  $\text{CO}_2$  and 19.5 vol.% of  $\text{H}_2\text{O}$

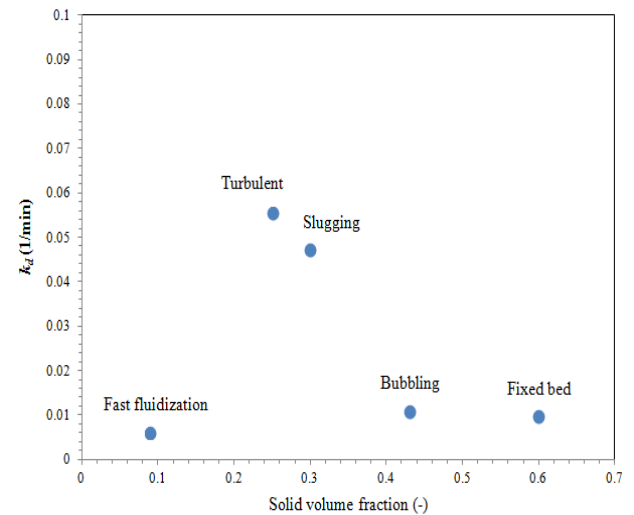
Although the fixed bed flow pattern gave the longest sorption result, the obtained value of  $k_0$  was very low. The solid sorbent packing among each other slows the speed of reaction rate. In bubbling fluidization regime, the value of  $k_0$  was slightly higher which is because of the high gas-solid sorbent mixing behavior. Considering the values of  $k_0$  for slugging and fast fluidization flow regimes, the similar  $k_0$  value range was observed due to the large bubble formation and low system residence time, respectively. The turbulent fluidization flow regime provided the highest value of  $k_0$  because of both the suitable residence time and system back-mixing [21]. In addition, the value of  $k_d$  or the deactivation rate constant had the same trend similar to the value of  $k_0$  or the initial sorption rate. For all the flow pattern/regimes, the  $k_d$  values were extremely lower than  $k_0$  values. This implies the low solid sorbent deactivation in all fluidization flow pattern/regimes causing by the solid sorbent properties and system hydrodynamics.

Finally, the solid volume fraction effect on the CO<sub>2</sub> sorption kinetic parameters was illustrated as shown in Figure 4. From the result in the figure, the highest kinetic parameters for the turbulent fluidization flow regime can be clarified using the appropriate solid sorbent concentration or volume fraction inside the system. The highest kinetic parameter was obtained at the moderate value of the solid concentration or volume fraction. At the low value, the solid particles were diluted and distributed across the column. At the high value, the solid particles were too dense inside the system and blocked the active surface area. Both the solid volume fraction behaviors then gave a negative effect on the sorption reaction rate.

To confirm the assumption for the derivation of the deactivation model, Figure 5 shows the SEM image taken at the magnification of x10000 (a) before and (b) after CO<sub>2</sub> sorption of Na<sub>2</sub>CO<sub>3</sub>/Al<sub>2</sub>O<sub>3</sub> solid sorbent in the turbulent fluidized bed. The surface image of the sorption product was distinctively different from the one of the reactant. After the CO<sub>2</sub> sorption, the layer of product over the solid sorbent was found.



(a)



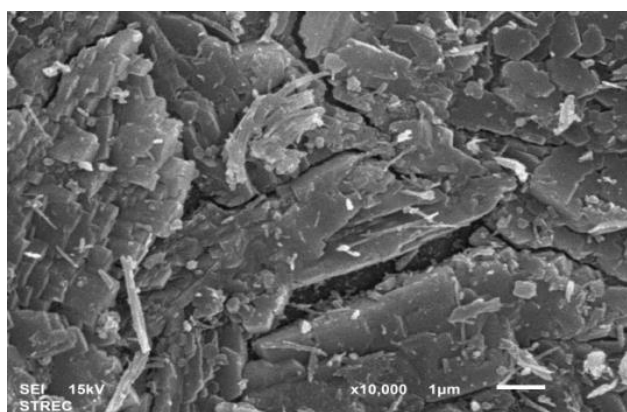
(b)

**Figure 4** The effect of the solid volume fraction on (a)  $k_0$  and (b)  $k_d$

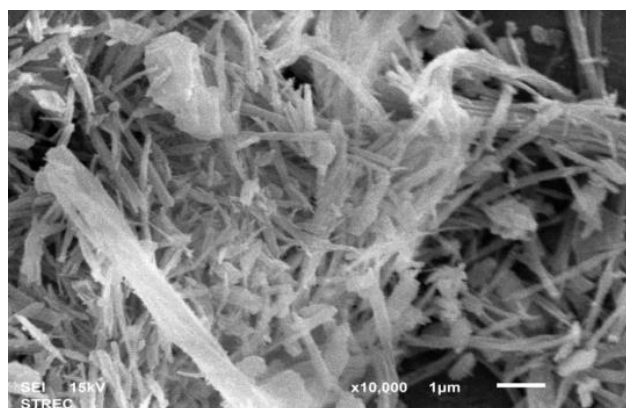
**Table 4** The effect of various flow regimes/flow patterns on initial sorption rate and deactivation rate at system temperature of 60°C and system pressure of 1 atm in 12 vol.% of CO<sub>2</sub> and 19.5 vol.% of H<sub>2</sub>O

Flow regime / flow pattern	W (g)	$k_0$ (m <sup>3</sup> /kg.min)	$k_d$ (1/min)	Solid volume fraction (-)
Fixed bed	40	0.1408	0.0098	0.60
Bubbling	40	0.1950	0.0108	0.43
Slugging	40	0.4979	0.0471	0.30
Turbulent	40	1.0934	0.0554	0.25
Fast fluidization	200	0.6020	0.0061	0.09





(a)



(b)

**Figure 5** SEM image taken at the magnification of  $\times 10000$  (a) before and (b) after  $\text{CO}_2$  sorption of  $\text{Na}_2\text{CO}_3/\text{Al}_2\text{O}_3$  solid sorbent in the turbulent fluidization regime at system temperature of  $60^\circ\text{C}$  and system pressure of 1 atm in 12 vol.% of  $\text{CO}_2$  and 19.5 vol.% of  $\text{H}_2\text{O}$

#### 4.0 CONCLUSION

The carbon dioxide sorption behavior and sorption kinetic parameters using deactivation kinetic model with sodium carbonate supported on alumina solid sorbent in fixed and fluidized bed reactors had been successfully investigated under different flow regimes/patterns. All the breakthrough curves were constant at the beginning stage then it decreased with the sorption time. The fixed bed flow pattern gave longest sorption time while the fast fluidized bed flow regime could not capture all the carbon dioxide concentration. The turbulent fluidized bed regime exhibited the highest value on carbon dioxide capture capacity. This can be explained by the sorption reaction rate constants were highest at moderate solid volume fraction value due to the suitable system hydrodynamics including the appropriate gas-solid sorbent contacting area and system residence time or solid sorbent elutriation.

It was found that the employed deactivation kinetic model was validated and fitted well with the obtained experimental data.

#### Acknowledgement

The 90th Anniversary of Chulalongkorn University Fund, the Ratchadaphiseksomphot Endowment Fund 2015 of Chulalongkorn University (CU-58-059-CC), the Faculty of Science of Chulalongkorn University and the Thailand Research Fund (TRG5780205) are acknowledged in this study.

#### References

- [1] Bandyopadhyay, A. 2014. *Carbon Capture and Storage: CO<sub>2</sub> Management Technologies*. CRC Press.
- [2] Chalermisinsuwan, B., Piumsomboon, P. and Gidaspow, D. 2010. A Computational Fluid Dynamics Design Of A Carbon Dioxide Sorption Circulating Fluidized Bed. *AIChE Journal*. 56: 2805-2824.
- [3] Zhao, C., Chen, X., Wu, Y. and Dong, W., 2012.  $\text{K}_2\text{CO}_3/\text{Al}_2\text{O}_3$  for Capturing  $\text{CO}_2$  In Flue Gas From Power Plants. Part 3:  $\text{CO}_2$  Capture Behaviors of  $\text{K}_2\text{CO}_3/\text{Al}_2\text{O}_3$  In A Bubbling Fluidized-Bed Reactor. *Energy & Fuels*. 26: 3062-3068.
- [4] Chaiwang, P., Chalermisinsuwan, B., Piumsomboon, P. and Gidaspow, D. 2014. CFD Design Of A Sorber For  $\text{CO}_2$  Capture With 75 And 375 Micron Particles. *Chemical Engineering Science*. 105: 32-45.
- [5] Jaiboon, O. A., Chalermisinsuwan, B., Mekasut, L. and Piumsomboon, P. 2013. Effect Of Flow Patterns/Regimes On  $\text{CO}_2$  Capture Using  $\text{K}_2\text{CO}_3$  Solid Sorbent In Fluidized Bed/Circulating Fluidized Bed. *Chemical Engineering Journal*. 219: 262-272.
- [6] Kunii, D., and Levenspiel, O. 1991. *Fluidization Engineering*. Butterworth-Heinemann.
- [7] Dong, W., Wu, Y., Zhao, C. and Liu C. L. 2012. Carbonation Characteristics Of Dry Sodium-Based Sorbents For  $\text{CO}_2$  Capture. *Energy & Fuels*. 26: 6040-6046.
- [8] Zhao, C., Chen, X., Zhao, C. 2010. Carbonation Behavior Of  $\text{K}_2\text{CO}_3$  With Different Microstructure Used As An Active Component Of Dry Sorbents For  $\text{CO}_2$  Capture. *Industrial & Engineering Chemistry Research*. 49: 12212-12216.
- [9] Khongprom, P. and Gidaspow, D. 2010. Compact Fluidized Bed Sorber For  $\text{CO}_2$  Capture. *Particology*. 8(6): 531-535.
- [10] Lee, S. C., Choi, B. Y., Lee, T. J., Ryu, C. K., Ahn, Y. S. and Kim, J. C. 2006.  $\text{CO}_2$  Absorption And Regeneration Of Alkali Metal-Based Solid Sorbents. *Catalysis Today*. 111: 385-390.
- [11] Dong, W., Chen, X., Yu, F. and Wu, Y. 2015.  $\text{Na}_2\text{CO}_3/\text{MgO}/\text{Al}_2\text{O}_3$  Solid Sorbents For Low-Temperature  $\text{CO}_2$  Capture. *Energy & Fuels*. 29(2): 968-973.
- [12] Liang, Y., Harrison, D. P., Gupta, R. P., Green, D. A. and McMichael, W. J. 2004. Carbon Dioxide Capture Using Dry Sodium-Based Sorbents. *Energy & Fuels*. 18(2): 569-575.
- [13] Arunkumar, S., Zhao, A., George K. H. S., Partha, S. and Rajender, G. 2012. Post-combustion  $\text{CO}_2$  Capture Using Solid Sorbents: A Review. *Industrial & Engineering Chemistry Research*. 51(4): 1438-1463.
- [14] Seo, Y., S. H., Ryu, H. J., Bae, H. D. and Yi, C. K. 2007. Effect Of Water Pretreatment On  $\text{CO}_2$  Capture Using A Potassium-Based Solid Sorbent In A Bubbling Fluidized Bed Reactor. *Chemical Engineering Journal*. 24: 457-460.
- [15] Park, S. W., Sung, D. H., Choi, B. S., Lee, J. W. and Kumazawa, H. 2006. Carbonation Kinetics Of Potassium Carbonate By Carbon Dioxide. *Journal of Industrial and Engineering Chemistry*. 12(4): 522-330.
- [16] Park, S. W., Sung, D. H., Choi, B. S., Oh, K. J. and Moon, K. H. 2006. Sorption Of Carbon Dioxide Onto Sodium Carbonate. *Separation Science and Technology*. 41: 2665-2684.
- [17] Park, S. W., Sung, D. H., Choi, B. S., Lee, J. W. and Kumazawa, H. 2009. Carbonation Kinetics Of Potassium Carbonate By Carbon Dioxide. *Korean Journal of Chemical Engineering*. 26(5): 1383-1388.
- [18] Zhao, C., Chen X. and Zhao, C. 2012. Carbonation Behavior And The Reaction Kinetic Of A New Dry Potassium-based

- Sorbent for CO<sub>2</sub> Capture. *Industrial & Engineering Chemistry Research*. 51: 14361-14366.
- [19] Lee, D. K., Young, D. M., Seo, H., Kang, N. Y., Choi, W. C. and Park, Y. K. 2013. Kinetic Expression For The Carbonation Reaction Of K<sub>2</sub>CO<sub>3</sub>/ZrO<sub>2</sub> Sorbent For CO<sub>2</sub> Capture. *Industrial & Engineering Chemistry Research*. 52(26): 9323-9329.
- [20] Guo, Y., Zhao, C. and Li, C. 2015. Thermogravimetric Analysis Of Kinetic Characteristics Of K<sub>2</sub>CO<sub>3</sub>-impregnated Mesoporous Silicas In Low-Concentration CO<sub>2</sub>. *Journal of Thermal Analysis and Calorimetry*. 121: 1393-1402
- [21] Jaiboon, O. A., Chalermisinsuwan, B., Mekasut, L. and Piumsomboon, P. 2013. Effect Of Flow Pattern On Power Spectral Density Of Pressure Fluctuation In Various Fluidization Regimes. *Powder Technology*. 233: 215-226.